

10A.2 IDEALIZED SIMULATIONS OF CIRCULATIONS FORCED BY LAND SURFACE HETEROGENEITY

Brian P. Reen*, David P. Tyndall, George S. Young, and David R. Stauffer
Penn State University, University Park, PA

1. INTRODUCTION

Bands of alternating vegetated and non-vegetated land (50-100 km wide) were found to enhance precipitation through mesoscale circulations in a two-dimensional analysis by Anthes (1984). Subsequent to that study many numerical studies (often idealized) have investigated the formation of circulations due to horizontal differences in surface heating (e.g., Yan and Anthes 1988; Chen and Avissar 1994; Patton et al 2005, Reen et al. 2006). Various names have been used to describe these circulations, but here the term inland breeze (Mahrt et al. 1994) is adopted.

Inland breezes are circulations that develop due to contrasts in surface buoyancy flux (SBF). The air above the larger SBF surface is warmer than the adjacent air over the smaller SBF surface; the resulting pressure gradient can create a near-surface wind that leads to a circulation. Inland breezes can result from SBF contrasts caused by factors that include (as noted by Segal and Arritt 1992) surface evapotranspiration (vegetation, soil wetness), subsurface thermal properties (sea surface temperature gradients, snowcover gradients, polar sea-ice openings), and reflection and absorption of solar radiance (clouds, surface albedo, atmospheric aerosols).

The strongest circulations have been found by many studies to occur when the heterogeneity is on the scale of about 100 km, the local Rossby radius for the planetary boundary layer (PBL; e.g., Chen and Avissar 1994; Lynn et al. 1995). Patton et al. (2005) found the strongest circulations occurred due to heterogeneity 4-9 times the depth of the PBL. However, the largest LES domain was only 30 km, precluding the representation of 100 km heterogeneity.

The effect of the background (synoptic) wind on the viability of inland breezes has been explored observationally (e.g. Doran et al. 1995; Mahrt et al. 1994) and numerically (Lynn et al. 1995; Avissar and Schmidt 1998). The synoptic wind needed to prevent the formation of an inland breeze varied by case in these studies. However, there seems to have been limited work to create an equation that uses factors such as synoptic wind to determine whether an inland breeze will form. A scale analysis by Mahrt et al. (1994) did address the relationship of variables to the formation of a circulation.

To investigate more rigorously the conditions in

which inland breezes form, we run idealized LES and mesoscale simulations using varied surface heating. This may lead to the ability to parameterize the effects of inland breezes not resolved by mesoscale simulations at a given model resolution. Section 2 provides the theoretical basis for the investigation, Section 3 is the model description, and Section 4 presents the experimental design for comparison simulations of which Section 5 presents results. Section 6 shows the results of a wider range of experiments, and Section 7 provides the summary and conclusions.

2. THEORY

The gravity current theory used by Qian et al. (1998) to model the movement of the rear of gust fronts can also be applied to inland breezes since both are solenoidal circulations affected by background wind. Applying their equation 2 to the case of an inland breeze caused by the difference in heating over a warm patch adjacent to a cool patch yields:

$$u_f = -k \sqrt{\frac{gz_i \Delta \theta_v}{\theta_v}} + C u_{syn} \quad (1)$$

where u_f is the speed of the lower-level flow in an absolute reference frame, k is the internal Froude number, g is the acceleration due to gravity, z_i is the PBL depth, $\Delta \theta_v$ is the difference in virtual potential temperature between the air over the warm patch and the air over the cool patch, θ_v is the virtual potential temperature of the air, u_{syn} is the synoptic wind speed perpendicular to the boundary between the warm patch and the cool patch, and C is a coefficient determining the strength of the synoptic wind's effect on the inland breeze. As in Qian et al. (1998), a value of 0.78 will be used for k as recommended by Simpson (1969). Qian et al. (1998) set C to 0.62 based on an analysis of Lucero (1983).

To calculate the synoptic wind speed necessary to exactly balance the inland breeze u_{tot} is set to zero. Setting u_{tot} to zero and converting to a flux-based formulation by approximating the advection time over the patch using only the synoptic wind and ignoring entrainment yields:

$$u_{syn} = \left(\frac{k}{C}\right)^{2/3} \left(\frac{Lg\Delta SBF}{\theta_v}\right)^{1/3} \quad (2)$$

where L is the size of the warm patch and ΔSBF is the difference in SBF between the warm patch and the cool patch. This can be rearranged into a non-dimensional group that determines the existence of an inland breeze

* Corresponding author address:

Brian P. Reen, 503 Walker Building, University Park, PA 16802; email: reenb@meteo.psu.edu

able to locally reverse the synoptic flow:

$$ND1 = \frac{\left(\frac{Lg\Delta SBF}{\theta_v} \right)^{1/3}}{u_{syn}} = \left(\frac{C}{k} \right)^{2/3} \quad (3)$$

Using the values of k and C used in Qian et al. (1998) yields a critical value of ~ 0.86 , with values larger than this resulting in inland breezes. This non-dimensional group can also be derived from Mahrt et al. (1994), whose scale analysis indicates a value of order one.

3. MODEL SETUP

For both the LES and the mesoscale model, the initial potential temperature profile is based on a sounding from 18 UTC 25 May 2002 at Homestead, Texas. There is no moisture in the simulations.

3.1 LES (CM1)

Large eddy-resolving simulations are performed using the Cloud-Resolving Model 1 (CM1), a compressible, non-hydrostatic, finite-differencing LES. A full description of the model may be found in Bryan and Fritsch (2002). The LES is run with periodic lateral boundary conditions in both the cross-wind and along-wind directions. The simulations run on a horizontal grid with 50 m x 50 m resolution and a stretched vertical grid with 20 m resolution near the surface and 40 m resolution above 1900 m. Horizontal domain width in the direction of heterogeneity is $2L$ for large patches (> 5 km) and $4L$ for small patches (< 5 km), while domain width in the direction of homogeneity is kept at 5 km. The domain extended to 3.5 km in the vertical. The model experiments are initialized with random temperature perturbations of ± 0.1 K at the lowest model level in order to initiate turbulent motions. Surface sensible heat flux is held constant during the simulations. No Coriolis effect is present in the LES runs considered below.

3.2 Mesoscale Model (WRF)

Idealized simulations of the Weather Research and Forecast Advanced Research WRF (WRF-ARW) model version 3.0.1.1 (Skamarock et al. 2008) are used for this study. No surface or atmospheric radiation scheme, cumulus parameterization, or moist physics is used.

The Mellor-Yamada-Janjic (MYJ) turbulent kinetic energy (TKE) scheme (Janjic 2001) and the accompanying Eta similarity surface layer model are used with some modification. First, the code to calculate surface sensible and latent heat fluxes is altered to allow for user-specified values of these quantities. Second, background TKE is decreased from 0.10 to 0.01 J kg^{-1} to better resolve low-TKE conditions. Thirdly, the PBL height diagnosed by the MYJ scheme was found to be significantly higher than that diagnosed based on the location of the capping inversion. For consistency with the LES PBL height calculation, PBL

height is diagnosed for use in the ND1 formulation from a technique based on the second derivative of potential temperature in the vertical.

Doubly periodic boundary conditions are used. There are 95 unstaggered vertical levels (half-levels), with 20-m resolution in the lowest 100 m and an average of ~ 30 -m resolution between 100 and 1000 m AGL. The model top is at 20 km.

In order to specify a chosen synoptic wind speed, an additional term is added to the wind tendency equation. This term mimics the imposition of a horizontal pressure gradient since in a doubly periodic simulation one cannot actually impose a uniform horizontal pressure gradient. If the desired wind field were merely imposed at the beginning of the simulation, the wind field would gradually decay due to surface friction. The chosen wind speed is used as the initial condition throughout the model domain but with adjustments near the surface using radix theory (Santoso and Stull 2001). The Coriolis effect is included with $f=1 \times 10^{-4} \text{ s}^{-1}$, consistent with a latitude of $\sim 45^\circ \text{ N}$.

4. EXPERIMENTAL DESIGN FOR COMPARISON SIMULATIONS

As illustrated in Figure 1, surface buoyancy flux (SBF) is specified as one value over half of the domain ("cool patch") and as a larger value over the other half of the domain ("warm patch"). The background wind, u_{syn} , flows across the heterogeneity.

Three experiments were designed such that the LES and the mesoscale model could both use the same domain size, patch size, background wind speed, etc. The domain is 32 km x 32 km, with 16 km wide cool and warm patches, and a background wind speed of 3 ms^{-1}

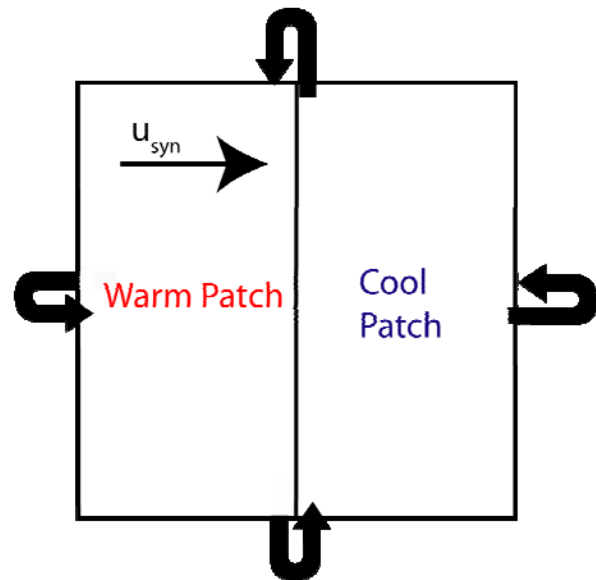


Fig. 1. Domain setup including periodic boundary conditions, surface sensible heat flux that is one value over the cool patch and a larger value over the warm patch, and a synoptic wind u_{syn} .

WRF uses 1 km horizontal resolution and CM1 uses 50 m horizontal resolution. The SBF over the cool patch is 0.01 K ms^{-1} for all experiments, but over the warm patch varies among experiments (0.11 K ms^{-1} for Exp. A, 0.16 K ms^{-1} for Exp. B, and 0.22 K ms^{-1} for Exp. C).

5. RESULTS FOR DIRECT COMPARISON SIMULATIONS

The effect of the thermal contrast on the component of the wind perpendicular to the heterogeneity for Exp. A is shown in Fig. 2. Compared to the background wind the wind over the cold patch is weaker near the surface and stronger near the PBL top at 2h for both models. The contrast between the colder air over the cool patch and the warmer air over the warm patch creates a pressure gradient that resists the background flow. In this case, the pressure gradient is not strong enough to overcome the background wind and reverse the flow. However, it is strong enough to create the signature of a circulation overlaid on the background flow, as demonstrated by the slowdown near the surface and the acceleration near the PBL top. One hour later at 3h, the circulation signature has been advected downwind in both models. By 4h, CM1 shows little evidence of a circulation overlaid on the background flow, while WRF still has evidence of this overlaid circulation. The ND1 for this experiment, calculated around 4h, is 1.26 for CM1 and 1.60 for WRF (Table 1). Most of the difference between these values is due to the larger wind speed within the PBL in CM1 compared to WRF. Although no closed circulation occurs in Exp. A, it is on the border since a closed circulation comes close to forming at 2h but then is washed out. Note that the PBL height is fairly similar between the two forecast models and does not change significantly in time, probably because of the PBL-top capping inversion strength.

Experiment B has a somewhat stronger SBF contrast (0.15 compared to 0.10 Kms^{-1} in Exp. A) and this is sufficient to cause a closed circulation to occur by 4h (Fig. 3). The flow reverses near the surface, with an area of $u < -1 \text{ ms}^{-1}$ in WRF, but in CM1 the reversed flow does not reach -1 ms^{-1} at 4h. In the return flow, however, CM1 has an area larger than 5 ms^{-1} but WRF never reaches this magnitude. The difference in the u component between the reversed flow and the return flow is similar in WRF and CM1 (5 ms^{-1}), but the u components themselves are $\sim 1 \text{ ms}^{-1}$ more positive in CM1 than WRF. This results in a larger value of ND1 for WRF (1.77) than CM1 (1.38).

Table 1. Comparison of CM1 and WRF experiments. “Circ formed” indicates whether a closed circulation formed.

Name	U_{init}	ΔSBF	ND1		Circ formed	
	ms^{-1}	Kms^{-1}	CM1	WRF	CM1	WRF
A	3.0	0.10	1.26	1.60	No	No
B	3.0	0.15	1.38	1.77	Yes	Yes
C	3.0	0.21	1.50	1.88	Yes	Yes

Experiment C has an even stronger SBF contrast (0.21 Kms^{-1}) and a result of this forms a stronger circulation with u reaching $< -2 \text{ ms}^{-1}$ (Fig. 3). Again, strength of the return flow is somewhat stronger in WRF (fairly large area $< -2 \text{ ms}^{-1}$) than CM1 (small area $< -2 \text{ ms}^{-1}$), but the return flow is stronger in CM1 (area of 6 ms^{-1} compared to only a small area of 5 ms^{-1} in WRF). This again results in a larger ND1 for WRF (1.88) than CM1 (1.50).

The vertical momentum flux also influences the development of circulations since a strong vertical momentum flux will tend to mix out circulations. Note that since a mesoscale model simulation does not explicitly resolve momentum flux, for WRF momentum flux based on the PBL parameterization is used. The LES, however, explicitly calculates scales which are not resolved in the mesoscale model. If the velocity field is decomposed into mean and fluctuating parts so that $u_i = U_i + u_i'$, the mesoscale model defines U_i as its resolved flow and u_i' as its unresolved flow. In order to calculate a comparable U_i from the LES data, a simple centered moving average of width equal to the mesoscale model grid cells is used to define U_i at each point, and $u_i' = u_i - U_i$. The perturbations u' and w' are then used to construct the momentum fluxes from the LES dataset. It is recognized that this method is an approximation and the momentum fluxes found in the mesoscale model and derived from the LES data are not defined identically. They are similar enough in meaning, however, that a qualitative comparison is possible.

A comparison of the vertical momentum flux between WRF and CM1 indicates that the magnitude of vertical momentum flux is generally similar but at a given time the similarity between WRF and CM1 in structure and magnitude varies. For example, the general structure and magnitude of vertical momentum flux are fairly similar in Exp. A at 2h (Fig. 4). At 3h the general structure and magnitude are also fairly similar, but there are differences such as the local minimum in WRF at $\sim 500 \text{ m}$ over the cool patch at $x \sim 25 \text{ km}$. The column of negative momentum flux in WRF at this location is consistent with the increase in u with height and the updraft associated with the overlaid circulation. In CM1 no such minimum at $\sim 500 \text{ m}$ is observed, though a weakly negative column of momentum flux does appear over the cold patch at $x \sim 25 \text{ km}$. By 4h, the vertical momentum flux is weakly correlated between WRF and CM1. The magnitude of vertical momentum flux is generally similar between WRF and CM1, indicating that WRF is not severely overmixing or undermixing momentum, both of which would strongly influence when circulations form. However, there is enough variability in the structure and exact magnitude of the vertical momentum fluxes that this may play a role in the difference between the critical value of ND1 in CM1 and WRF (Table 1).

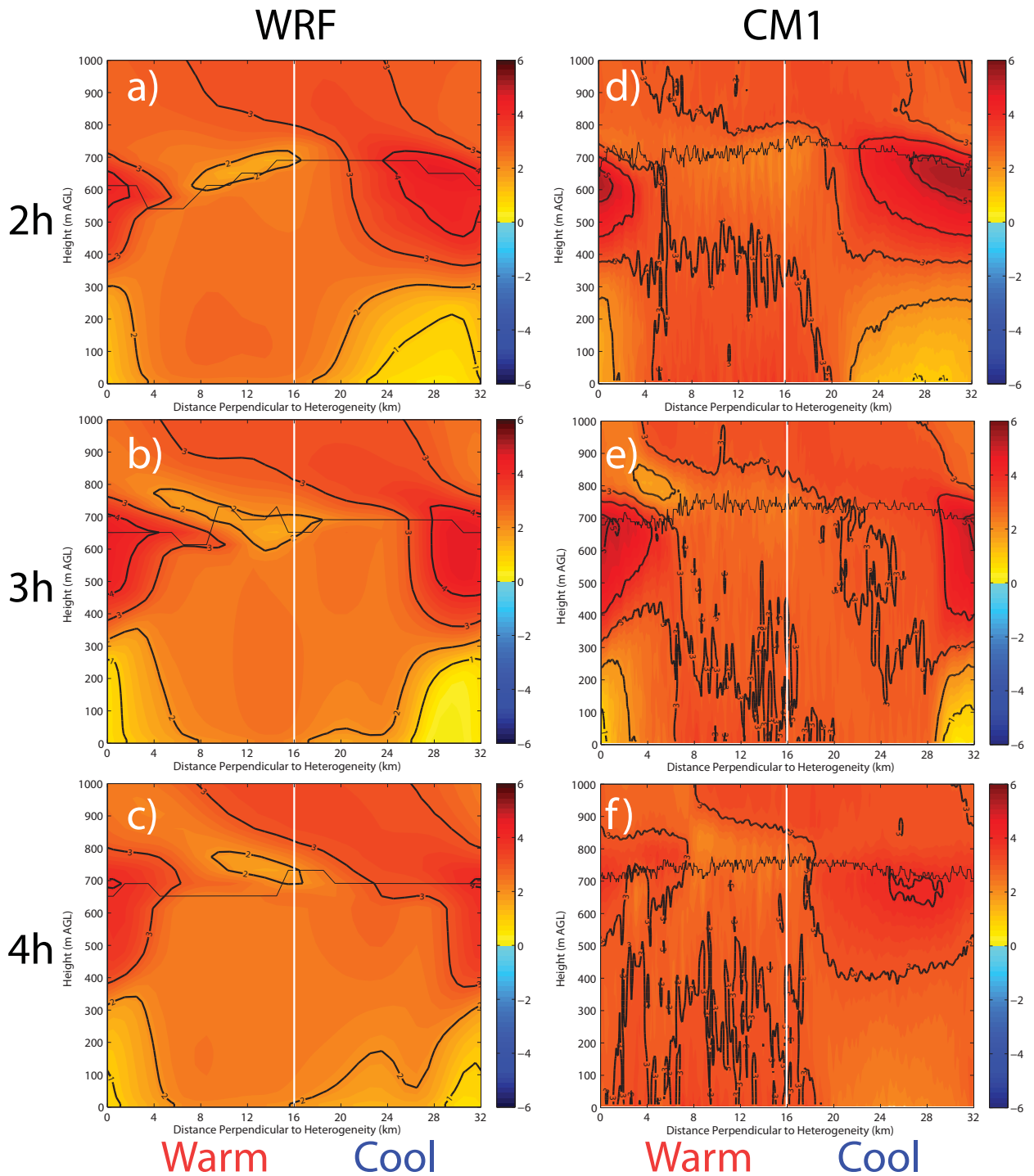


Fig. 2. Component of wind (ms^{-1}) perpendicular to heterogeneity averaged in the homogeneous direction for Exp. A at $t=2, 3,$ and 4h in WRF (a-c) and CM1 (d-f). In order to reduce the influence of thermals, LES fields have been averaged over a 15-minute period ending with the stated time. This 15-minute period corresponds to approximately twice the convective timescale of the warm patch. Thick black lines are contour lines every 1 ms^{-1} and the thin black line is the PBL top. The vertical white line is the border between the warm patch and the cool patch.

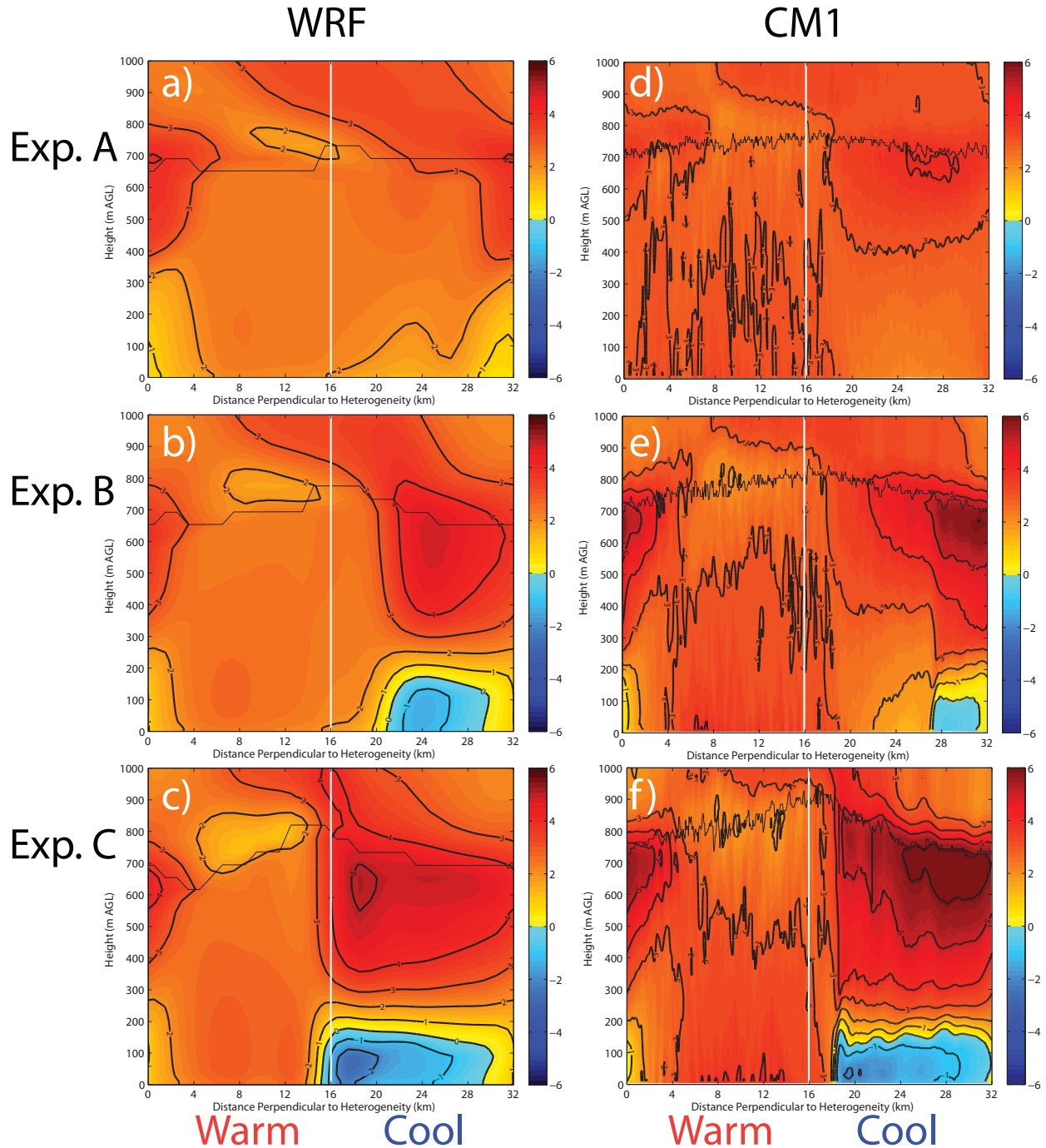


Fig. 3. Component of wind (ms^{-1}) perpendicular to heterogeneity averaged in the homogeneous direction for Exps. A, B, and C in WRF (a-c) and CM1 (d-f) at $t=4\text{h}$. In order to reduce the influence of thermals, LES fields have been averaged over a 15-minute period ending with the stated time. This 15-minute period corresponds to approximately twice the convective timescale of the warm patch in Exps. A and B and 2.5 times the convective timescale of the warm patch in Exp. C. Thick black lines are contour lines every 1 ms^{-1} and the thin black line is the PBL top. The vertical white line is the border between the warm patch and the cool patch.

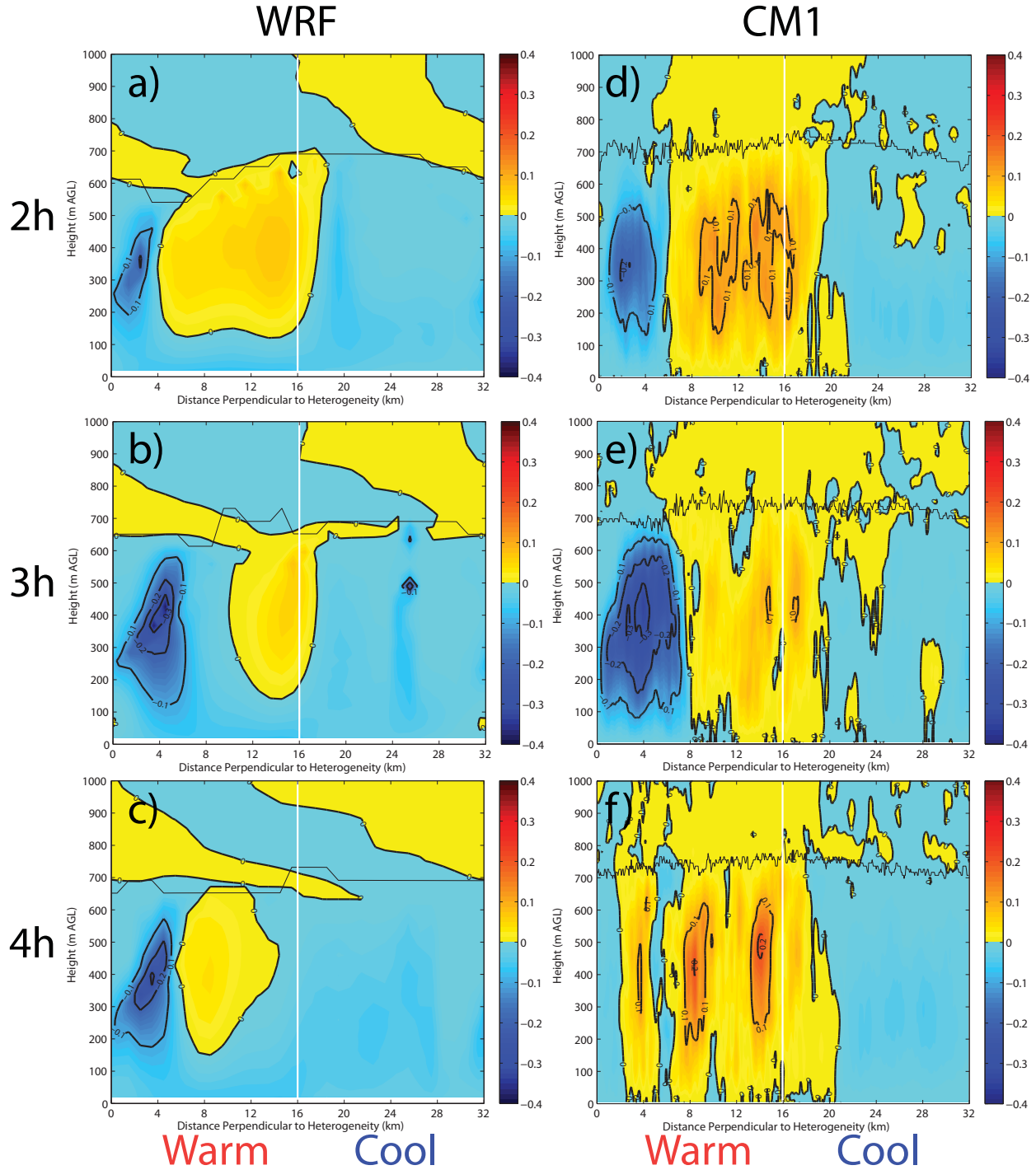


Fig. 4. Vertical momentum flux (m^2s^{-2}) averaged in the homogeneous direction for Exp. A at $t=2, 3,$ and 4h in WRF (a-c) and CM1 (d-f). In order to reduce the noise due to thermals, LES fields have been averaged over a 15-minute period ending with the stated time, and a simple central moving average of radius 500 m has been applied. The 15-minute period corresponds to approximately twice the convective timescale of the warm patch in Exp. A. Thick black lines are contour lines every $0.1 \text{ m}^2\text{s}^{-2}$ and the thin black line is the PBL top. The vertical white line is the border between the warm patch and the cool patch.

6. ND1 EXPERIMENTS

Many experiments are carried out in WRF that do not have an equivalent experiment in CM1, and vice versa. Because of the minimum scales resolvable in a mesoscale model and the computational restraints of a large domain in LES, smaller domains are more suited to CM1 and larger domains to WRF. The experiments varied in SBF contrast (CM1 from 0.01 to 0.21 Kms^{-1} and WRF from 0.01 to 0.393 Kms^{-1}) and background wind (CM1 from 0.5 to 5.5 ms^{-1} and WRF from 2.0 to 9.5 ms^{-1}). For CM1 the patch size (1.5 to 16.0 km) also varied while in WRF this was constant (56 km). The horizontal resolution for these experiments was 50 m in CM1 and 4 km in WRF. Fig. 5 shows whether a circulation forms or not in ND1 vs. ND2 space for WRF and CM1 experiments with a cool patch SBF of 0.01 Kms^{-1} . ND2 is the ratio of advective and convective timescales. A large value of ND2 indicates that it takes much longer to advect across the warm patch compared to the timescale of a thermal.

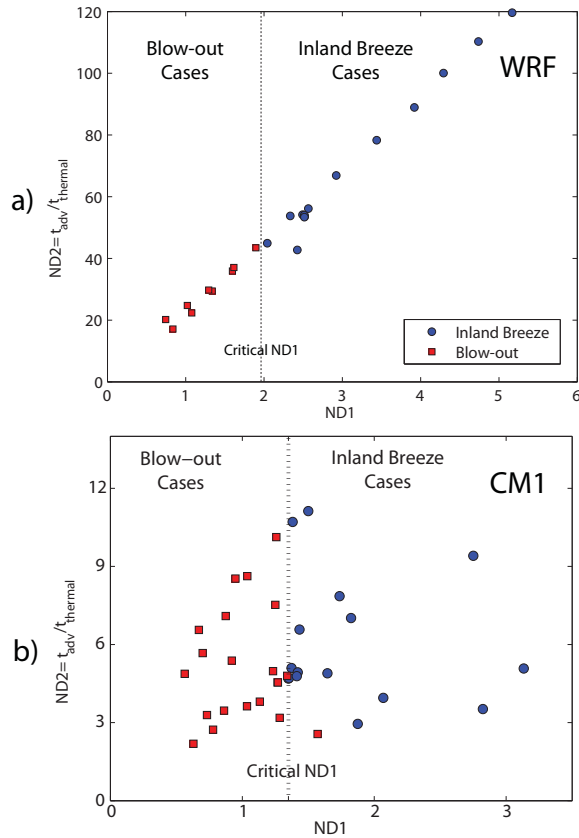


Fig. 5. Phase diagram of the non-dimensional group ND1 versus ND2 for a) WRF and b) CM1 experiments. Blue circles indicate model experiments where a closed circulation forms (inland breeze) and red squares indicate model experiments where the background wind is too strong to allow a closed circulation to form (Blow-out).

In these cases ND1 is a good predictor of whether a closed circulation will form. For values greater than ~ 1.3 a circulation forms, while for values less than ~ 1.3 the background wind is strong enough to “blow out” the circulation and prevent it from forming. For WRF the critical value is just less than 2.0. Having a larger critical value of ND1 in WRF compared to CM1 is consistent with Exps. A-C discussed in the prior section. However, the value of this critical value in WRF is between 1.60 and 1.77 in Exps. A-C, somewhat smaller than the 2.00 for the experiments in Fig. 5. This may be related to the smaller size of the warm and cool patches in Exps. A-C than the WRF experiments in Fig. 5.

Other experiments (not shown) change the value of SBF over the cool patch (in contrast to the single value of cool patch SBF used in Fig. 5). These experiments have indicated that the critical value of ND1 is also dependent on the cool patch SBF. This may be due to the increased vertical mixing over the cool patch.

7. SUMMARY AND CONCLUSIONS

A formulation to predict whether a closed circulation will form with a given surface heat flux contrast has been proposed. This formulation was tested in three experiments in LES (CM1) and the mesoscale model (WRF) using very similar model configurations. These experiments indicated that WRF and CM1 agree on whether a circulation forms in each case, but that the values of ND1 associated with parallel runs differ. This difference is largely due to differences in the PBL mean wind speed. This difference in ND1 between parallel WRF and CM1 experiments results in different critical values for the two models. The differences in vertical momentum flux and heat flux between WRF and CM1 are being examined to better understand the variability in the critical value of ND1 in these experiments. CM1 experiments using the Coriolis effect are planned to make Exps. A-C in CM1 more consistent with the parallel WRF experiments.

Many model experiments were completed in WRF that did not have a parallel run in CM1, and vice versa. Both WRF and CM1 indicated that the existence of a closed circulation is dependent on the nondimensional group ND1. However, the value of this threshold varied between the WRF and CM1. The direct comparison experiments A-C are being used to better understand this difference in threshold values between WRF and CM1.

Other experiments not shown here indicate a potential dependence on cool patch SBF, a factor not included in ND1. Efforts are underway to account for the effect of the cool patch SBF.

Further analysis of the differences between parallel CM1 and WRF experiments are underway to further understand the differences between these two types of models. In addition to investigating how to predict whether a circulation will form, this research may ultimately lead to a method for parameterization of unresolved inland breezes in mesoscale models.

8. ACKNOWLEDGMENTS

The flux specification WRF modifications were based on code provided by Mariusz Pagowski (NOAA/ESRL). This research was supported by DTRA W911NF-06-1-0439 under the supervision of Dr. John Hannan.

9. REFERENCES

- Anthes, R. A., 1984: Enhancement of convective precipitation by mesoscale variations in vegetative covering in semiarid regions. *J. Clim. Appl. Meteor.*, **23**, 541-553.
- Avissar, R., and T. Schmidt, 1998: An evaluation of the scale at which ground-surface heat flux patchiness affects the convective boundary layer using large-eddy simulations. *J. Atmos. Sci.*, **55**, 2666-2689.
- Bryan, G. H. and J. M. Fritch, 2002: A benchmark simulation for moist nonhydrostatic numerical models. *Mon. Wea. Rev.*, **130**, 2917-2928.
- Chen, F. and R. Avissar, 1994: The impact of land-surface wetness heterogeneity on mesoscale heat fluxes. *J. Appl. Meteor.*, **33**, 1323-1340.
- Doran, J. C., W. J. Shaw, and J. M. Hubbe, 1995: Boundary layer characteristics over areas of inhomogeneous surface fluxes, *J. Appl. Meteor.*, **34**, 559-571.
- Grell, G. A., J. Dudhia, and D. R. Stauffer, 1995: A description of the fifth-generation Penn State / NCAR Mesoscale Model (MM5), NCAR/TN-398+STR, NCAR, Boulder, CO, 122 pp.
- Janjic, Z. I., 2001: Nonsingular implementation of the Mellor-Yamada level 2.5 scheme in the NCEP meso model. *NCEP Office Note*, **No. 437**, 61 pp. [Available online: <http://www.emc.ncep.noaa.gov/officenotes/newernote/s/on437.pdf>]
- Lucero, O. A., 1983: Behavior and characteristics of storm cold outflows. Ph.D. thesis, University of Virginia, 191 pp. [Available from Dept. of Environmental Sciences, University of Virginia, Charlottesville, VA 22903.]
- Lynn, B. H., D. Rind, and R. Avissar, 1995: The importance of mesoscale circulations generated by subgrid-scale landscape heterogeneities in general circulation models. *J. Climate*, **8**, 191-205.
- Mahrt, L., J. Sun, D. Vickers, J. I. MacPherson, J. R. Pederson, R. J. Desjardins, 1994: Observations of fluxes and inland breezes Over a heterogeneous surface. *J. Atmos. Sci.*, **51**, 2184-2499.
- Patton, E. G., P. P. Sullivan, and C.-H. Moeng, 2005: The influence of idealized heterogeneity on wet and dry planetary boundary layers coupled to the land surface. *J. Atmos. Sci.*, **62**, 2079-2097.
- Qian, L., G. S. Young, and W. M. Frank, 1998: A convective wake parameterization scheme for use in general circulation models. *Mon. Wea. Rev.*, **126**, 456-469.
- Reen, B. P., D. R. Stauffer, K. J. Davis, and A. R. Desai, 2006: A case study on the effects of heterogeneous soil moisture on mesoscale boundary-layer structure in the Southern Great Plains, U.S.A. Part II: mesoscale modelling. *Bound.-Layer Meteor.*, **120**, 275-314.
- Santoso, E., and R. Stull, 2001: Similarity equations for wind and temperature profiles in the radix layer, at the bottom of the convective boundary layer. *J. Atmos. Sci.*, **58**, 1446-1464.
- Segal, M. and R. W. Arritt, 1992: Nonclassical mesoscale circulations caused by surface sensible heat-flux gradients. *Bull. Amer. Meteor. Soc.*, **73**, 1593-1604.
- Simpson, J. E., 1969: A comparison between laboratory and atmospheric density currents. *Quart. J. Roy. Meteor. Soc.*, **95**, 758-765.
- Skamarock, W. C., J. B. Klemp, J. Dudhia, D. O. Gill, D. M. Barker, M. G. Duda, X.-Y. Huang, W. Wang, and J. G. Powers, 2008: A description of the advanced research WRF Version 3. *NCAR Tech Note*, **NCAR/TN-475+STR**, 113 pp. [Available online: http://www.mmm.ucar.edu/wrf/users/docs/arw_v3.pdf]
- Yan, H., and R. A. Anthes, 1988: The effect of variations in surface moisture on mesoscale circulations. *Mon. Wea. Rev.*, **116**, 192-20.